

Article

Synthesis of Copper-Substituted Polyoxovanadate and Oxidation of 1-Phenyl Ethanol

Isshin Yoshida ^{1,*}, Ryoji Mitsuhashi ², Yuji Kikukawa ^{1,*}  and Yoshihito Hayashi ^{1,*} 

¹ Department of Chemistry, Graduate School of Natural Science and Technology, Kanazawa University, Kakuma, Kanazawa 920-1192, Japan; isshin5564@stu.kanazawa-u.ac.jp

² Institute of Liberal Arts and Science, Kanazawa University, Kakuma, Kanazawa 920-1192, Japan; mitsuhashi@staff.kanazawa-u.ac.jp

* Correspondence: kikukawa@se.kanazawa-u.ac.jp (Y.K.); hayashi@se.kanazawa-u.ac.jp (Y.H.)

Abstract: Dicopper-substituted polyoxovanadate $[\text{Cu}_2\text{V}_{16}\text{O}_{44}(\text{NO}_3)]^{5-}$ (Cu2V16) was synthesized through the reaction of $[\text{Cu}_2\text{V}_8\text{O}_{24}]^{4-}$ and $[\text{V}_4\text{O}_{12}]^{4-}$ in the presence of nitrate salt. From single crystal X-ray analysis, Cu2V16 exhibited the same helical structure as that of nitrate-incorporated polyoxovanadate, $[\text{V}_{18}\text{O}_{46}(\text{NO}_3)]^{5-}$ (V18). Both complexes had the same framework with the same guest anion and are considered to be substituted isomers for each other by replacing two Cu^{2+} ions and two $[\text{VO}]^{2+}$ ions. The incorporated nitrate showed short and long N–O bond lengths (1.14, 1.26 and 1.30 Å) as in the case of V18 (1.09, 1.16 and 1.28 Å). Reflecting the inequivalent bond lengths of the nitrate, the IR spectrum of V18 shows split peaks at 1359 and 1342 cm^{-1} . But the Cu2V16 spectrum showed a single peak due to the presence of nitrate at 1353 cm^{-1} . When the temperature was lowered, the nitrate peak in Cu2V16 was split into two positions at 1354 and 1345 cm^{-1} when the temperature reached -140 °C. These results indicate that the nitrate incorporated in Cu2V16 rotates relatively easily in the Cu2V16 cavity at room temperature compared to V18. In addition, the oxidation of 1-phenyl ethanol to acetophenone with Cu2V16 smoothly proceeded in comparison with V18. By taking advantage of the same framework in both catalysts, we can deduce the position of potential active sites in the oxidation reaction. We have concluded that the most active site is not on the peripheral of the vanadate framework, but it is reasonable to suggest that the active site is on the substituted copper atoms rather than the polyoxovanadate framework.

Keywords: polyoxovanadates; metal-substitution; nitrate; alcohol oxidation; supra-ceramics



Citation: Yoshida, I.; Mitsuhashi, R.; Kikukawa, Y.; Hayashi, Y. Synthesis of Copper-Substituted Polyoxovanadate and Oxidation of 1-Phenyl Ethanol. *Inorganics* **2024**, *12*, 61. <https://doi.org/10.3390/inorganics12020061>

Academic Editors: László Kótai and Lukáš Krivosudský

Received: 18 January 2024

Revised: 6 February 2024

Accepted: 17 February 2024

Published: 19 February 2024



Copyright: © 2024 by the authors. Licensee MDPI, Basel, Switzerland. This article is an open access article distributed under the terms and conditions of the Creative Commons Attribution (CC BY) license (<https://creativecommons.org/licenses/by/4.0/>).

1. Introduction

Metal-oxygen cluster anions of early transition metals are called polyoxometalates. They exhibit well-defined molecular structures that are characterized by spectroscopic analysis and/or X-ray diffraction technique. They have received attention in various research fields, such as electrochemistry, catalysts, magnetochemistry, photochemistry, and biochemistry [1–4]. Polyoxotungstates and polyoxomolybdates exhibit various metastable structures such as Keggin, Wells–Dawson, Anderson, Preysler, and Keplerate-type structures. For the purpose of the addition and improvements of each property, the immobilization of a heterometal cation in the polyoxometalate structure has been studied as one of the promising approaches [5,6]. For instance, through an incorporation of paramagnetic metal cations into a polyoxometalate framework, various types of magnetic materials are reported. Another example includes an alternation of redox properties by incorporating a constituent element, through which the cations acted as stable shuttle redox mediators [7,8]. In addition, the HOMO and/or LUMO gap is also adjusted by inserting a heterometal cation for the purpose of developing a unique photocatalyst system [9]. In the case of polyoxotungstates and polyoxomolybdates, some established methods to synthesize a heterometal-core-containing polyoxometalates were reported. The synthesis of metal substituted polyoxometalates

may be categorized within the following two methods [10]. One-pot synthesis is a typical method to incorporate a hetero metal into the framework: the acid-condensation reaction achieved by mixing an oxo metal species such as Na_2WO_4 or Na_2MoO_4 with Na_2HPO_4 , and/or Na_2SiO_3 , followed by the reaction with $\text{M}(\text{NO}_3)_x$, and/or MCl_x (M: transition metal cations) as a source of metal-substituted sites, gave a polyoxometalate indicating that a parent framework is partly substituted by the introduced transition cations. Although this method is easy to carry out, it is difficult to predict the resulting structure formed in the reaction, and the optimization of the reaction is difficult because it tends to produce potential isomers in the solution. The other synthetic method is stepwise synthesis. Under an appropriate condition, by carefully adjusting the pH, some units of polyoxotungstates or polyoxomolybdates are dissociated to give a specific lacunary-type derivative. The lacunary-type polyoxometalates act as inorganic ligands and can be coordinated to transition metal cations. The traditional synthesis of heterometal-incorporated polyoxometalates has been carried out in aqueous media. The recent development of the synthesis in non-aqueous media made it possible to control the hydrolysis reaction and contributed to achieve a rational design of new polyoxometalates. Now, the synthesis of polyoxometalates with a hetero-multinuclear core at a specific site has been well established [11].

Vanadium-based polyoxometalates in the name of polyoxovanadates show a structure versatility, and a correlation between the structure and property has been discussed [12,13]. Until now, various metal-containing polyoxovanadates have been reported [12–25]. Our group and Streb's group have developed VO_4 -based polyoxovanadates [13–15]. The utilization of the high nucleophilicity of tetrahedral VO_4 of the vertex-sharing polyoxovanadate ring enables one to stabilize various kinds of transition metal cations at the center of the inorganic ring structure. The valence state of the vanadium atoms with the tetrahedral coordination geometry in the reported polyoxovanadate rings is 5+. Until now, a series of transition metal cations such as V^{4+} (square pyramidal coordination geometry), Mn^{2+} , Mn^{3+} , Mn^{4+} , Co^{2+} , Ni^{2+} , Cu^{2+} , Zn^{2+} , Y^{3+} , Pd^{2+} , La^{3+} , Ce^{3+} , Pr^{3+} , Nd^{3+} , Sm^{3+} , Eu^{3+} , Gd^{3+} , Tb^{3+} , Dy^{3+} , Ho^{3+} , Er^{3+} , Tm^{3+} , Yb^{3+} , and Lu^{3+} were stabilized at the center of polyoxovanadate rings as an inorganic macrocyclic complex. In many cases, the number of VO_4 units and their ring conformations are flexible enough to fit in a different ionic radius of the incorporated hetero metal cation. The polyoxovanadate macrocyclic ring, $[\text{VO}_3]_n^{n-}$, has a flexible ring size and conformation by adjusting the V–O–V bond angles and altering the ring size through dissociation and association of the $[\text{VO}_3]^-$ unit. An appropriate ring structure was produced until it fit the radius of a metal cation. The dissociation and association of the $[\text{VO}_3]^-$ unit has been reported in $[\text{V}_4\text{O}_{12}]^{4-}$: the equilibrium between $[\text{V}_3\text{O}_9]^{3-}$ and $[\text{V}_4\text{O}_{12}]^{4-}$ is observed in acetonitrile solution [26]. The series of Lanthanide-containing polyoxovanadates have been observed in a different ring size according to the ionic radii of a lanthanide cation: the larger lanthanide ion has been adopted in a larger polyoxovanadate ring. These previous examples are considered to be inorganic macrocyclic complexes of a transition metal cation coordinated by a multi-membered polyoxovanadate cyclic ligand. In these precedented examples, a metal cation was incorporated at the center of the ring. Instead of the incorporation of a metal unit in the structure, a substitution of polyoxometalate parent framework is also possible. $[\text{Cu}_2\text{V}_8\text{O}_{24}]^{4-}$ is an example of “metal-substituted” polyoxovanadates in that two V=O units in $[\text{V}_{10}\text{O}_{26}]^{4-}$ structure are substituted with two Cu^{2+} ions (Figure 1). Matson's group has developed heterometallic VO_6 -based Lindqvist type polyoxovanadates [16–18]. Metal-substituted VO_6 -based polyoxovanadates, such as $[\text{PtV}_9\text{O}_{28}]^{7-}$, $[\text{MoV}_9\text{O}_{28}]^{5-}$, and $[\text{MnV}_{12}\text{O}_{34}]^{4-}$, were also reported [19–21]. Streb's group has developed a chemistry of VO_5 -based polyoxovanadate, $[\text{V}_{12}\text{O}_{32}(\text{Cl})]^{4-}$ [22–25]. A unique tube-type structure has two open sites at both ends on the tube, where various kinds of metal cations were able to stabilize. The oxygen atoms at the terminal position on the tube peripheral may coordinate to the cations as if the cation was capping the tube. These complexes with a different capping metal cation may be considered substituted isomers. In the sense of the coordination ability, the tube-type polyoxovanadate can be

considered one of the lacunary-type polyoxometalates, but corresponding fully occupied polyoxovanadates have not been reported yet.

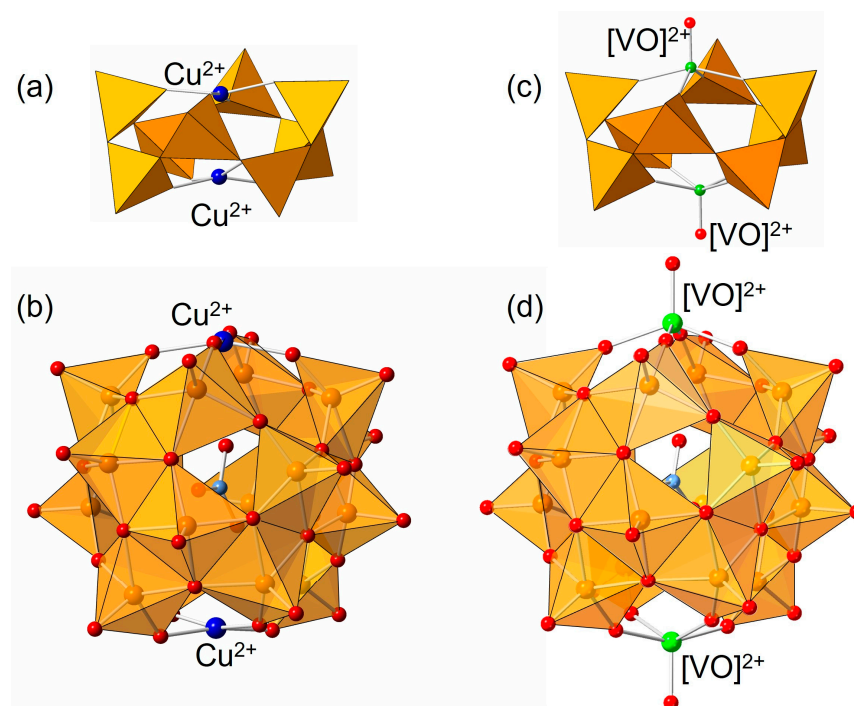


Figure 1. Structure comparison of the substituted complexes between (a) $[\text{Cu}_2\text{V}_8\text{O}_{24}]^{4-}$ and (c) $[\text{V}_{10}\text{O}_{26}]^{4-}$, and between (b) $[\text{Cu}_2\text{V}_{16}\text{O}_{44}(\text{NO}_3)]^{5-}$ and (d) $[\text{V}_{18}\text{O}_{46}(\text{NO}_3)]^{5-}$. The structural relationship is considered to be a substitution of two Cu^{2+} to two $[\text{V}=\text{O}]^{2+}$ units. The blue, green, red, and light blue spheres represent Cu^{2+} , V^{4+} , oxygen, and nitrogen atoms, respectively. Orange polyhedra represent tetrahedral $\text{V}^{\text{V}}\text{O}_4$ or square pyramidal $\text{V}^{\text{V}}\text{O}_5$ units.

In other words, the tube-type dodecavanadates are a unique structural unit that is slightly different from the category of “metal-substituted” polyoxovanadates that may be defined as a complex with substituted transition metal cations in a polyoxovanadate framework. Semimetal-oxygen species also exist on the surface of various VO_5 -based polyoxovanadates [27]. The unique feature of VO_5 -based polyoxovanadates is a formation of a hollow spherical structure. Because polyoxovanadates have a structural versatility based on the flexible number of vanadium atoms, various kinds of anion were included in the cavity with a different size of a spherical structure to incorporate a particular guest anion. For example, anions such as F^- , Cl^- , Br^- , I^- , NO_3^- , ClO_4^- , NO^- , NO_2^- , N_3^- , AcO^- , OCN^- , and NO_2^- were stabilized at the center of a spherical polyoxovanadate. Interestingly, the shape of the cavity highly depends on the shape of the anion inside the sphere due to the freedom of the arrangement of VO_5 units with a different angle. Since the property of the polyoxometalates depends on the structures, the precise comparison among different derivatives is necessary to understand the difference of the property. As shown above, compared with polyoxotungstates and polyoxomolybdates, the synthesis of “metal-substituted” polyoxovanadates is still developing due to its lability, and the development of a new methodology is required to prevent the formation of complicated isomeric mixtures in the course of synthesis [13].

In the current synthesis of a metal-substituted polyoxovanadate, there are two issues: one is the number of heterometals introduced in the main framework tends to vary to give a mixture of mono-substituted complex, di-substituted complex, tri-substituted complex and so on, despite a stoichiometric control of a metal source for the substitution. The second issue is that as the number of substituted metal atoms increases, the number of possible positional isomers increases significantly, and it becomes very difficult to purify

and separate those different complexes. To avoid the above issues, we planned a synthesis through a polyoxovanadate framework-expansion reaction using the insertion of well-established metavanadates, $[V_4O_{12}]^{4-}$, into a smaller spherical polyoxovanadate that was already isolated as disubstituted isomers. Nitrate-incorporated polyoxovanadate $[V_{18}O_{46}(NO_3)]^{5-}$ (V18) possesses two reduced hetero-atom units, $[V^{IV}O]^{2+}$ at the top and bottom, supported by a V16 polyoxovanadate belt framework where all vanadium atoms are in the +5 valence state. The original synthesis included the overoxidation of $[V_{10}O_{26}]^{4-}$ in the presence of NO_3^- [28]. Recently, a new polyoxovanadate, $[V_{10}O_{24}]^{2-}$, was reported by using the thermal treatment of the well-known $[H_3V_{10}O_{28}]^{3-}$ as a precursor to produce V18 [29]. The formation of V18 with two different procedures indicate that V18 is a thermodynamically (meta)stable species in the presence of NO_3^- . With the latter procedure, a different substituent was introduced in the framework in the presence of Cu^{2+} or Ca^{2+} . The starting material of the first procedure, $[V_{10}O_{26}]^{4-}$, possessed two $[V^{IV}O]^{2+}$ on the top and bottom in a V_8O_{24} ring (Figure 1). Among the various VO_4 -based metal-containing polyoxovanadates, Cu-containing polyoxovanadate, $[Cu_2V_8O_{24}]^{4-}$, also exhibits a similar structure as that of $[V_{10}O_{26}]^{4-}$ (Figure 1). Here, the $[VO]^{2+}$ sites of the square-pyramidal $V^{IV}O_5$ units in $[V_{10}O_{26}]^{4-}$ were substituted with square planar Cu^{2+} ions. We utilize this structural resemblance to synthesize a larger VO_5 -based copper-substituted polyoxovanadate. In this work, a new synthetic route of V18 from $[V_{10}O_{26}]^{4-}$ without a redox process was investigated, and copper-substituted polyoxovanadate was synthesized from $[Cu_2V_8O_{24}]^{4-}$ instead of $[V_{10}O_{26}]^{4-}$. The comparison of structures, thermal properties, and catalytic performance for alcohol oxidation were also investigated.

2. Results and Discussion

The positions of two heteroatom units, $[V^{IV}O]^{2+}$, in the smallest spherical polyoxovanadate, $[V_{10}O_{26}]^{4-}$, are on opposite sides of each other or in a trans position, capping both ends of V8 belt structure (Figure 1c). There is not enough space to hold a guest ion at the center of $[V_{10}O_{26}]^{4-}$. When we compared the structural relationship between $[V_{10}O_{26}]^{4-}$ and $[V_{18}O_{46}(NO_3)]^{5-}$ (V18), we found a structural similarity between those two different polyoxovanadates. V18 is a larger spherical structure than V10. The V16 belt in V18 may be reconstructed by twisting the V8 belt in V10 into a helix, and adding another eight vanadium units on the opposite side of the helix belt in a shape of the double helix may complete the V18 structure from V10 after including a nitrate anion at the expanded center. The advantage of this retrosynthesis has two parts: (i) the stereospecific position of two hetero atom units $[V^{IV}O]^{2+}$ remain in the trans-position and (ii) the stoichiometry of the substituted hetero atom units stays exactly the same (two units), avoiding the complication of the formation of many different isomers in a different substitution number. Simple polyoxovanadates $[V_4O_{12}]^{4-}$ were selected to insert two units of the V4 framework, since $[V_4O_{12}]^{4-}$ easily link to each other to expand the ring sizes in a different number. The formation of a longer vanadium belt by dimerization of V4 units is feasible in polyoxovanadate chemistry. To the acetonitrile solution of $\{^nBu_4N\}_4[V_{10}O_{26}]$, 2 equiv. of $\{^nBu_4N\}_4[V_4O_{12}]$ were added. Then, NO_3^- as a template anion was introduced to ensure the formation of a V16 belt unit. The addition of 8 equiv. of *p*-toluene sulfonic acid (TsOH) with respect to $[V_{10}O_{26}]^{4-}$ was performed to complete the acid-condensation reaction (ex. 1).



With the addition of diethyl ether, the green precipitates were obtained by filtration. The successive washing with tetrahydrofuran (THF) to remove $\{^nBu_4N\}TsO$ gave the powder of V18 in a 86% yield. The IR spectrum of the obtained powder was identical to that of the original V18, showing that V18 is able to be synthesized by using an acid/base reaction without the redox process.

We also tested this framework expansion reaction to synthesize a copper-substituted polyoxovanadate (Cu2V16). In this case, the valence state of all vanadium atoms is at its highest oxidation state V(V). To the acetonitrile solution of $\{^nBu_4N\}_4[Cu_2V_8O_{24}]$, 2 equiv. of

$\{\text{nBu}_4\text{N}\}_4[\text{V}_4\text{O}_{12}]$, $\{\text{nBu}_4\text{N}\}\text{NO}_3$ and 8 equiv. of *p*-toluene sulfonic acid (TsOH) were added as a one-pot reaction. The reaction formula was expected as follows (ex 2),



The electrospray-ionization mass spectrum of the products showed the main signal sets at $m/z = 1702$ and 3162 due to $\{\{\text{nBu}_4\text{N}\}_7\text{Cu}_2\text{V}_{16}\text{O}_{44}(\text{NO}_3)\}^{2+}$ and $\{\{\text{nBu}_4\text{N}\}_6\text{Cu}_2\text{V}_{16}\text{O}_{44}(\text{NO}_3)\}^+$, respectively (Figure S1). These results show that the formula of the product is $\{\text{nBu}_4\text{N}\}_5[\text{Cu}_2\text{V}_{16}\text{O}_{44}(\text{NO}_3)]$. The Vis/NIR spectrum shows no significant peaks over 600 nm, suggesting the absence of V^{4+} in the products (Figure 2) because a mixed valence complex always shows intense bands due to intervalence charge transfer (IVCT). In the case of a mixed valence V18 complex, the Vis/NIR spectrum shows a strong broad band in the region of 600–1500 nm (Figure 2), confirming the presence of V(IV) inherited from the starting complex. The comparison of the cyclic voltammogram between Cu2V16 and V18 shows that two redox pairs from the reversible redox at the cap parts of the double helical belts in V18 disappear in the voltammogram of Cu2V16 (Figure S2). The $E_{1/2}$ values of V18 observed at -0.41 , -0.77 , and -1.35 V were negatively shifted to -0.50 , -0.84 , and -1.42 V in Cu2V16 by the effect of the substitution of two copper ions. The magnetic susceptibility measurement of Cu2V16 was carried out (Figure S3). The $\chi_{\text{m}}T$ products linearly decreased upon cooling, indicating the presence of temperature-independent paramagnetism ($7 \times 10^{-4} \text{ cm}^3 \text{ mol}^{-1}$). Upon further cooling, the $\chi_{\text{m}}T$ products abruptly dropped with the weak antiferromagnetic interactions. Although the $\chi_{\text{m}}T$ value of $0.96 \text{ cm}^3 \text{ K mol}^{-1}$ at 300 K was slightly larger than the spin-only value expected for two Cu^{2+} ion (0.75), the magnetic data were fully consistent with those expected for Cu2V16.

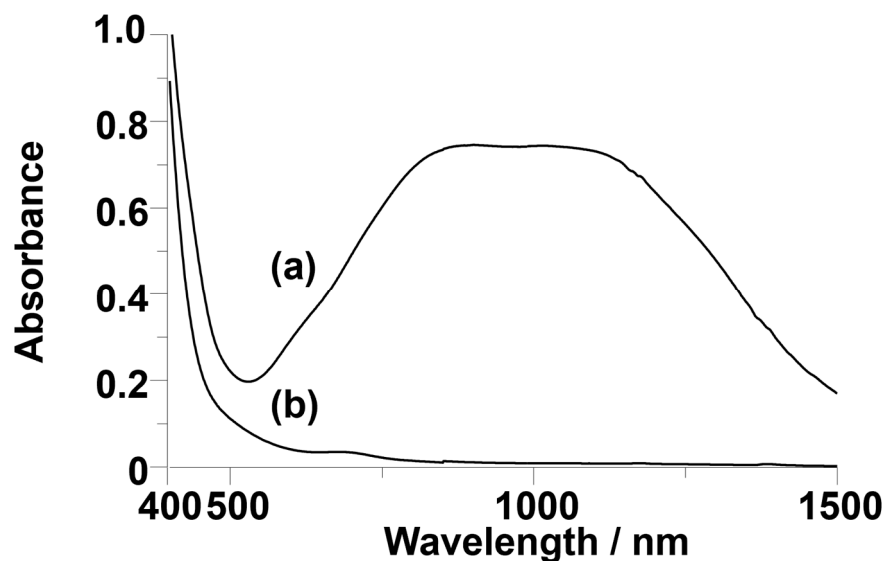


Figure 2. Vis/NIR spectra of (a) V18 and (b) Cu2V16 in acetonitrile. The concentration of the samples was 0.2 mM. The broad band around 600–1500 nm is due to intervalence charge transfer.

The thermogravimetric analysis (TGA) showed the plateau between 100 °C and 150 °C at 0.64% weight loss (Figure S4). This value suggests that the tetra-*n*-butyl ammonium salts of Cu2V16 possess one hydration water. The large weight loss over 200 °C was due to the decomposition of tetra-*n*-butyl ammonium cations. The elemental analysis also supported the chemical formula of the obtained compound as $\{\text{nBu}_4\text{N}\}_5[\text{Cu}_2\text{V}_{16}\text{O}_{44}(\text{NO}_3)] \cdot \text{H}_2\text{O}$. This is the first report on copper-containing helical polyoxovanadates, as far as we know.

The single crystals suitable for the X-ray analysis were obtained by the cation-exchange reaction to the tetramethyl ammonium cations (Table S1). The crystal system was monoclinic, and the space group was $P2_1/c$. The unit parameter and the volume were the moderate values among the polyoxometalates. Five tetramethyl ammonium cations were

observed per one anion, showing that the charge of the observed anion is 5[−]. The anion structure was almost the same as that of the original helical V18. The top and bottom cap parts on the helix were confirmed as copper atoms. At the axial position of one of the copper atoms, acetonitrile was solvated with a distance of 2.41 Å. At the axial position of the other side of copper atom, a terminal oxygen atom from the neighboring Cu2V16 anion interacted at a distance of 2.64 Å. These distances are too large to consider as a chemical bond. Therefore, the coordination geometry of copper atoms is considered to be pseudo-square pyramidal. The double helix part in the body of Cu2V16 was identical to that of the original V18. The N–O distances from an incorporated nitrate showed a variation of bond lengths as short and longer bonds. The N–O bond length perpendicular to the hypothetical line connecting two copper atoms was 1.144 Å, and the rest of the N–O bond lengths were 1.260 and 1.301 Å (Table 1). A similar set of bond lengths is also observed in V18 (1.090, 1.157, and 1.284 Å). The angle of the guest nitrate triangle from the line between the capped atoms of Cu2V16 was ca. 12°. This value is also the same as that of V18 (Figure 3). The distances between the capped copper atoms of Cu2V16 and vanadium atoms of V18 were 7.70 and 8.55 Å, respectively, showing that the cavity size of the spherical skeleton of Cu2V16 was smaller than that of V18 (Table 1). The bond lengths between the copper atoms and the surrounding oxygen atoms were 1.894, 1.905, 1.923, and 1.935 Å and 1.904, 1.907, 1.916, and 1.920 Å, respectively (Table 1). From the bond valence sum values of copper (2.12 and 2.13) and vanadium (4.98–5.19), the valences of copper and vanadium were identified as +2 and +5, respectively [30]. This result was also supported by the observation of the Vis/NIR spectrum (no presence of V⁴⁺) and the magnetic susceptibility (presence of two Cu²⁺) results.

Table 1. Selected distances (Å) observed in the crystal structures ¹.

	Cu2V16	V18 [22]
Cu1–O30, V16–O18	1.935(4)	1.903(4)
Cu1–O36, V16–O16	1.894(4)	1.902(4)
Cu1–O40, V16–O17	1.923(4)	1.905(4)
Cu1–O34, V16–O19	1.905(4)	1.910(4)
Cu2–O1, V17–O25	1.920(4)	1.919(4)
Cu2–O2, V17–O27	1.904(4)	1.903(4)
Cu2–O3, V17–O26	1.907(4)	1.898(4)
Cu2–O4, V17–O28	1.916(4)	1.921(4)
Cu1...Cu2, V16...V17	7.70	8.55
N101–O101, N1–O47	1.144(10)	1.090(10)
N101–O102, N1–O49	1.301(10)	1.284(18)
N101–O101, N1–O48	1.260(10)	1.157(16)

¹ The geometrically corresponding positions between the two anion structures in crystallographic analysis are compared.

The IR spectrum of Cu2V16 was somewhat different from that of the original V18 (Figure S5). The peak positions were almost the same, while the intensity was different, probably due to the difference of the number of V=O and V–O–V fragments. The signals due to NO₃[−] were also different. The original V18 shows the two peaks at 1359 and 1342 cm^{−1} due to NO₃[−] [28]. The reason why two peaks were observed can be explained from the information provided by crystallographic analysis. In the crystal structure of V18, the N–O bond that is vertical to the line connecting two [VO]²⁺ cap parts was shorter than the others. Although the chemical environment of NO₃[−] of Cu2V16 at −183 °C is identical to that of V18, the IR spectrum of Cu2V16 shows the single N–O vibration peak at 1351 cm^{−1}, indicating that nitrate bond lengths in Cu2V16 are thermally averaged at room temperature. To analyze the degree of nitrate rotation in these complexes, IR spectra were measured at various low temperatures. When decreasing the temperature, the single peak at 1353 cm^{−1} at room temperature assigned as nitrate stretching was gradually split while the peaks due to the Cu2V18 skeleton itself were maintained (Figure 4). When the

surface temperature of the IR cell reached $-140\text{ }^{\circ}\text{C}$, the two peaks at 1354 and 1345 cm^{-1} were observed even in the $\text{Cu}_2\text{V16}$ complex as we expected. These results indicate that the mobility of the nitrate anion was different between $\text{Cu}_2\text{V16}$ and the original V18. This is explained by assuming that a nitrate in $\text{Cu}_2\text{V16}$ is rotated easily at room temperature, while that in V18 is fixed without rotation due to the interaction with the main framework through a strong trans influence of the square pyramidal VO_5 units [31]. Mobility or orientation control of molecular fragments in the polyoxometalates caused the polarity change of the compound. Recently, the polarity control of polyoxometalates has gained attention [32]. By changing the position of the metal cations between two stable sites in the Preysler-type polyoxometalate, the single-molecule electret property was observed at temperatures above room temperature.

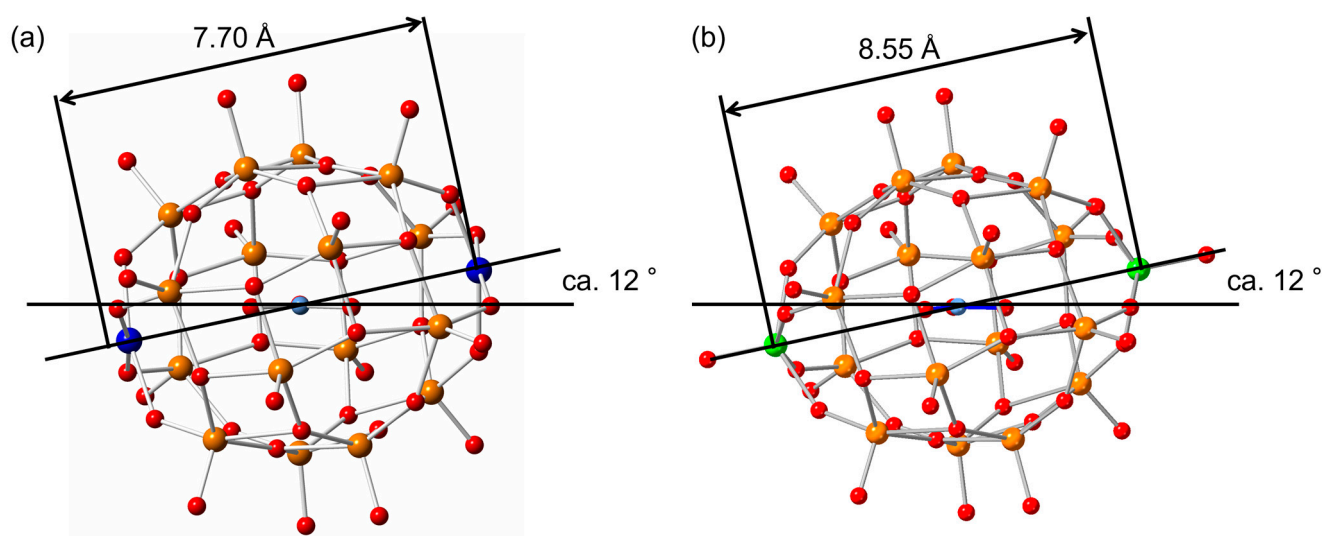


Figure 3. Ball-and-stick representations of (a) $\text{Cu}_2\text{V16}$ and (b) V18. Orange, blue, green, red, and light blue spheres represent pentavalent vanadium, tetravalent vanadium, copper, oxygen, and nitrogen atoms, respectively.

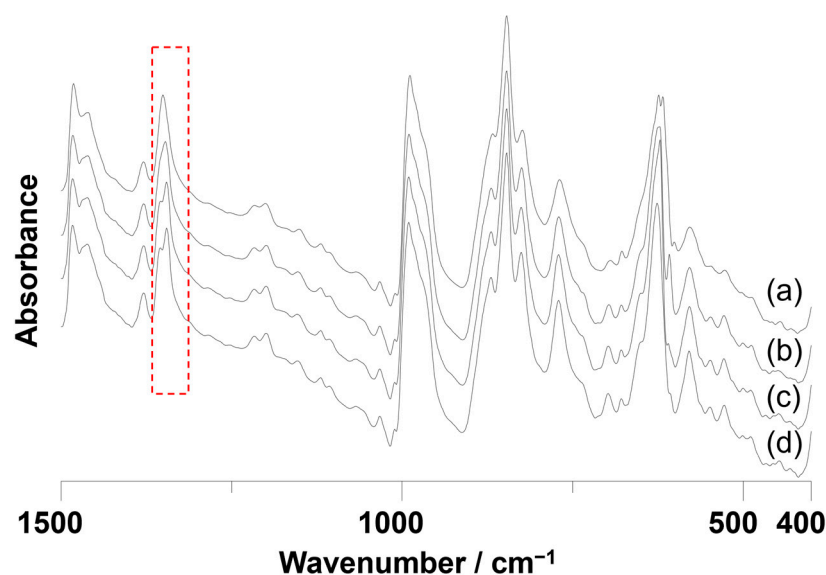


Figure 4. IR spectra of $\text{Cu}_2\text{V16}$ at (a) $20\text{ }^{\circ}\text{C}$, (b) $-60\text{ }^{\circ}\text{C}$, (c) $-110\text{ }^{\circ}\text{C}$, and (d) $-140\text{ }^{\circ}\text{C}$. The highlighted region represents the signals due to NO_3^- in $\text{Cu}_2\text{V16}$.

By taking advantage of the isomeric structural relationship between $\text{Cu}_2\text{V16}$ and V18, we conducted the oxidation reaction to deduce where an active site is on the cluster framework. The comparison of the oxidation catalytic performance was investigated

between Tetra-*n*-butyl ammonium salts of Cu2V16 and V18. The 1-phenyl ethanol oxidation with tert-butyl hydroperoxide (TBHP) as an oxidant was carried out (Table 2). In the presence of 5 μmol of Cu2V16, 1-phenyl ethanol was converted to acetophenone with 77% yield in 24 h. The turnover number reached 154, and the turnover frequency was 6.4 h^{-1} . The yields with 5 μmol of V18 and without catalysts were only 6% and 2% under the same reaction conditions, respectively. When we tested a catalytic performance of 10 μmol of $\text{Cu}(\text{NO}_3)_2$ as a control, the yield was observed in 20%, indicating that Cu^{2+} has a potential to act as a catalytic center for this reaction. The control reaction with both of the starting materials for Cu2V16 and V18 was also investigated. With $[\text{nBu}_4\text{N}]_4[\text{Cu}_2\text{V}_8\text{O}_{24}]$, the oxidation products were obtained in 69%. This value was significantly higher than that of $[\text{nBu}_4\text{N}]_4[\text{V}_{10}\text{O}_{26}]$. The starting material of V18 that is $[\text{nBu}_4\text{N}]_4[\text{V}_{10}\text{O}_{26}]$ was decomposed during the reaction.

Table 2. Catalytic oxidation of 1-phenyl ethanol to acetophenone ^{1,2}.

Entry	Catalysts (μmol)	Yield (%)
1	Cu2V16 (5) ³	77
2	V18 (5)	6
3	$\text{Cu}(\text{NO}_3)_2$ (10)	20
4	$[\text{nBu}_4\text{N}]_4[\text{Cu}_2\text{V}_8\text{O}_{24}]$ (5)	69
5	$[\text{nBu}_4\text{N}]_4[\text{V}_{10}\text{O}_{26}]$ (5) ⁴	31
6	Blank	2

¹ Reaction conditions; 1-phenyl ethanol 1 mmol, 5.5 M TBHP in decane 1 mmol, catalyst 5 or 10 μmol , acetonitrile 2 mL at 32 $^\circ\text{C}$, 24 h under Ar atmosphere. ² Yield was determined by GC with internal standard method. ³ Tetra-*n*-butyl ammonium salts were utilized. ⁴ The complex was decomposed during the reaction.

With the addition of an excess amount of diethyl ether into the reaction solution after the oxidation reaction with Cu2V16 and V18, precipitated catalysts were recovered by filtration. The IR spectra of the catalysts after the reaction were identical to those of the authentic samples, showing that the structures of Cu2V16 and V18 are maintained during the reactions (Figure S6). From these results and the same helical structure of Cu2V16 as that of V18, the active sites may be concluded at substituted copper sites. The low steric hindrance around square planar Cu^{2+} may allow the easy approach of the reactants because the axial position of the square planer copper site is coordinatively unsaturated, while the access on the polyoxovanadate framework is hindered by the presence of terminal oxygen atoms sticking out from the spherical framework that is disturbing the approach of the reactant on a vanadium atom.

3. Materials and Methods

Methods: The electrospray ionization mass spectra were recorded on a JEOL JMS-T100TD (JEOL Ltd., Tokyo, Japan). The IR spectra were measured on a Jasco FT/IR-4200 (Jasco Inc., Tokyo, Japan) using a KBr method. Temperature-dependent IR spectra were measured on a Jasco FT/IR-6600 using the transmission method with a sample-coated Si disk in a gas-cell made of glass under a vacuum. The sample-coated Si disk was prepared with the evaporation of acetonitrile after dropping an acetonitrile solution of tetra-*n*-butyl ammonium salts of Cu2V16 on the surface of the Si disk. For the window of the gas-cell, Si disks were used. The gas-cell was cooled by the flow of liquid nitrogen through the rolled SUS tube on the surface of the cell. The temperature was measured by the thermocouple set on the surface of the gas-cell. The cyclic voltammetry was carried out using a Biologic SP-50 instrument (BioLogic, Grenoble, France) by using a standard

three-electrode cell with a glassy carbon electrode, a Pt counter electrode, and a Ag/Ag⁺ reference electrode. The electrodes were purchased from Bioelectro Analytical Science (BAS) Inc. (Eatonville, WA, USA). Elemental analyses of C, H, and N were performed by the Research Institute for Instrumental Analysis at Kanazawa University. Elemental analyses of V and Cu were performed by a Thermo Fisher Scientific inductively coupled plasma atomic emission spectroscopy iCAP6300 (Thermo Fisher Scientific, Waltham, MA, USA). The Vis/NIR spectra were measured on a Jasco V-770. Thermogravimetry data were collected on a Rigaku Thermo plus EVO2 instrument (Rigaku, Cedar Park, TX, USA) with a temperature sweep rate of 10 °C/min under 0.2 L/min N₂ flow. GC analysis was performed on a Shimadzu GC-2014 (Shimadzu, Tokyo, Japan) with a flame ionization detector (FID) equipped with a ZB-WAXplus capillary column (phenomenex, internal diameter = 0.25 mm, length = 30 m). Naphthalene was used as an internal standard. Magnetic measurements were performed with a MPMS3 SQUID magnetometer (Quantum Design, San Diego, CA, USA). The polycrystalline sample was grounded into fine powder and loaded into a gelatin capsule. All data were corrected for diamagnetism of the sample by means of Pascal's constant [33]. Temperature dependence of magnetic susceptibility was fitted using the PHI program, version 3.1.6 [34]. The distillation of a small amount of reagent was performed by using a glass tube oven of a SIBATA GTO-1000 (SIBATA, Tokyo, Japan).

X-ray Crystallography: Single-crystal structural analysis of Cu₂V₁₆ was performed at −183 °C with a Bruker D8 VENTURE diffractometer with Cu-Kα radiation (λ = 1.54178 Å). The data reduction and absorption correction were completed using the APEX3 program [35]. The structural analyses were performed using APEX3 and winGX for Windows software [36]. The structures were solved by SHELXT (direct methods) and were refined by using SHELXL-2018 [37]. Non-hydrogen atoms were refined anisotropically. Hydrogen atoms were positioned geometrically and were refined using a riding model. Crystallographic data are summarized in Table S1. CCDC 2322749 contains the supplementary crystallographic data for this paper. These data can be obtained free of charge from The Cambridge Crystallographic Data Centre via www.ccdc.cam.ac.uk/data_request/cif.

Reagents: Vanadium(IV) oxide sulfate hydrate, acetonitrile, diethyl ether, ethyl acetate, tetrahydrofuran and tetra-*n*-butyl ammonium nitrate, triethylamine were purchased from FUJIFILM Wako Pure Chemical Corporation. In addition, 40% tetra-*n*-butyl ammonium hydroxide in water and 5.5 M *tert*-butyl hydroperoxide in decane solution were purchased from Sigma-Aldrich. Vanadium oxide, naphthalene, and acetophenone were purchased from Tokyo Chemical Industry Co., Ltd., Tokyo, Japan. *p*-Toluene sulfonic acid was purchased from KANTO CHEMICAL Co., Inc. (Tokyo, Japan). These chemicals were used as received without further purification. Copper nitrate trihydrate was purchased from Fujifilm Wako Pure Chemical Corporation (Tokyo, Japan) and used after the recrystallization. 1-Phenyl Ethanol was obtained from Fujifilm Wako Chemicals Corporation and used after distillation by a glass tube oven. In addition, 5.5 M *tert*-butyl hydroperoxide solution in decane was obtained from Sigma-Aldrich. {ⁿBu₄N}₄[Cu₂V₈O₂₄], {ⁿBu₄N}₄[V₁₀O₂₆] and {ⁿBu₄N}₄[V₄O₁₂] were prepared based on the previously reported procedures [38–40].

Synthesis of [V₁₈O₄₆(NO₃)]^{5−}: First, 31.4 mg of {ⁿBu₄N}₄[V₁₀O₂₆], 45.6 mg of {ⁿBu₄N}₄[V₄O₁₂], and 5.1 mg of {ⁿBu₄N}NO₃ were dissolved in 2 mL of acetonitrile. Then, 25.4 mg of *p*-toluene sulfonic acid was dissolved in 1 mL of acetonitrile. The two solutions were mixed. The reaction solution was refluxed for 48 h. To the dark green solution, the addition of an excess amount of diethyl ether gave the green precipitates. The precipitates were collected by filtration, washed with tetrahydrofuran, and dried to give 41.7 mg of the products (86.0% yield). IR: 2960, 2932, 2873, 1483, 1464, 1383, 1360, 1342, 1151, 1106, 1062, 993, 874, 839, 784, 630, 570 cm^{−1}.

Synthesis of [Cu₂V₁₆O₄₄(NO₃)]^{5−}: First, 31.4 mg of {ⁿBu₄N}₄[Cu₂V₈O₂₄], 45.6 mg of {ⁿBu₄N}₄[V₄O₁₂], and 51 mg of {ⁿBu₄N}NO₃ were dissolved in 2 mL of acetonitrile. Then, 25.4 mg of *p*-toluene sulfonic acid was dissolved in 1 mL of acetonitrile. The two solutions were mixed and refluxed for 3.5 h. To the dark brown solution, the addition of an excess amount of diethyl ether gave the brown precipitates. The precipitates were collected by fil-

tration, washed with tetrahydrofuran, and dried to give 44.7 mg of the products (92.1% yield based on $[\text{Cu}_2\text{V}_8\text{O}_{24}]^{4-}$). Elemental analysis calcd (%) for $(^n\text{Bu}_4\text{N})_5[\text{Cu}_2\text{V}_{16}\text{O}_{44}(\text{NO}_3)]\cdot\text{H}_2\text{O}$ ($\text{C}_{80}\text{H}_{182}\text{Cu}_2\text{N}_6\text{O}_{48}\text{V}_{16}$): C, 32.70; H, 6.24; N, 2.86; Cu, 4.33; V, 27.74. Found: C, 32.34; H, 6.08; N, 2.81; Cu, 4.61; V, 28.30. IR: 2962, 2933, 2873, 1484, 1464, 1384, 1354, 1216, 1200, 1153, 1121, 1104, 1060, 1034, 993, 871, 852, 828, 771, 632, 582 cm^{-1} . The thermogravimetric analysis (TGA) showed 0.64% weight loss at 130 °C (Figure S4). This value was almost equal to the weight loss of the one hydrated water from the calculated formula. Single crystals suitable for X-ray analysis were obtained by addition of $(\text{Me}_4\text{N})\text{BF}_4$ to the acetonitrile solution of $(^n\text{Bu}_4\text{N})_5[\text{Cu}_2\text{V}_{16}\text{O}_{44}(\text{NO}_3)]$.

Oxidation of 1-phenyl ethanol: First, 1-phenyl ethanol 1 mmol, catalyst 5 or 10 μmol , acetonitrile 2 mL, and naphthalene 0.2 mmol (internal standard) were put in the test tube with a screw cap. The solution was kept at 32 °C under Ar atmosphere. The solution was stirred at 800 rpm with the Teflon-coated magnetic stir bar at 32 °C. The reaction started with the addition of 5.5 M TBHP in decane solution 1 mmol to the reaction solution. Yield was determined by GC with the internal standard method. The products were determined by the retention time of the commercially available authentic chemicals. After 24 h, an excess amount of diethyl ether was added to the reaction solution and the precipitates were collected by filtration and dried. The collected solid was characterized by IR spectroscopic analysis (Figure S6).

4. Conclusions

Either $[\text{V}_{10}\text{O}_{26}]^{4-}$ where two vanadium ions are reduced to V(IV) or $[\text{Cu}_2\text{V}_8\text{O}_{24}]^{4-}$ in which two vanadium sites are substituted to Cu^{2+} is considered to be in a relationship of a substituted isomer to each other by replacing two $[\text{VO}]^{2+}$ ions with two Cu^{2+} cation or vice versa. By utilizing those starting materials, we successfully developed the sphere expansion reaction to give $[\text{V}_{18}\text{O}_{46}(\text{NO}_3)]^{5-}$ and dicopper-substituted polyoxovanadate $[\text{Cu}_2\text{V}_{16}\text{O}_{44}(\text{NO}_3)]^{5-}$ selectively without a redox process in the synthesis. This new synthetic method achieved the stereospecific alternation of the polyoxometalate framework by means of a positional isomer in the substitution reaction, and the insertion of vanadium units to expand a spherical polyoxovanadate framework is a new method of synthesis avoiding an extremely difficult purification procedure through a formation of a complicated mixture of various substituted isomers in the synthesis of polyoxometalates. To obtain the designed polyoxometalates, the strategy of the synthetic procedure is important. Although the spheric cavity in the helical Cu_2V_{16} was smaller than that of V18, the encapsulated nitrate in Cu_2V_{16} rotated more smoothly than that of V18. The larger cavity of V18 allows nitrate to interact with the main framework, resulting in fixing the position of the nitrate, while the small cavity size of Cu_2V_{16} did not allow arranging the nitrate in the best position; rather, it floats in the cavity, which makes thermal rotation easier at room temperature. Both complexes have the same framework in the relationship of substituted isomers with each other, and the comparison of the catalytic reactivity allows us to estimate the position of an active site in the oxidation reaction. As a result, the catalytic performance of Cu_2V_{16} was higher than that of V18. The comparative study of the catalytic reactivity between two substituted isomers emphasizes the importance of a transition metal cation introduced on a polyoxometalate framework by the substitution reaction. In this work, racemic catalysts were used. After the optical resolution of these Cu_2V_{16} and V18 complexes, the enantio-selective oxidation by inorganic oxide molecules without using organic ligands is expected. In addition, since $[\text{V}_{10}\text{O}_{26}]^{4-}$ is one of the precursors to obtain various kinds of polyoxovanadates, synthesis of other copper-substituted polyoxovanadates is also expected in the near future.

Supplementary Materials: The following supporting information can be downloaded at: <https://www.mdpi.com/article/10.3390/inorganics12020061/s1>, Table S1: Crystallographic data for Cu_2V_{16} ; Figure S1: Electrospray-ionization mass spectra of Cu_2V_{16} in acetonitrile; Figure S2: Cyclic voltammogram of (a) Cu_2V_{16} and (b) V18 in acetonitrile; Figure S3: $\chi_m T$ versus T plot of Cu_2V_{16} ; Figure S4: Thermogravimetric data of Cu_2V_{16} ; Figure S5: IR spectra of (a) tetramethyl ammonium salts of

Cu2V16, (b) tetra-*n*-butyl ammonium salts of Cu2V16, and (c) V18; Figure S6: IR spectra of (a) V18 before the catalytic reaction, (b) V18 after the catalytic reaction, (c) Cu2V16 before the catalytic reaction, and (d) Cu2V16 after the catalytic reaction.

Author Contributions: Conceptualization, temperature-dependent IR, X-ray analysis, Y.K.; Magnetic susceptibility measurement, R.M.; other experimental investigation, data correction, I.Y. supervision, Y.H.; funding acquisition, Y.K. All authors have read and agreed to the published version of the manuscript.

Funding: This research was partly supported by JSPS KAKENHI Grand Number JP23H04621 and JP23K04776, JSPS Core-to-Core program, JST FOREST Program Grant Number JPMJFR2023720466.

Data Availability Statement: The data presented in this study are available in article and the supplementary materials.

Acknowledgments: We thank Y. Nakazato for the preliminary experiments. The magnetic measurements were conducted in Institute of Molecular Science, supported by ARIM of MEXT (Project: JPMXP1223MS1015).

Conflicts of Interest: The authors declare no conflicts of interest.

References

1. Hill, C.L. Themed issue on polyoxometalates. *Chem. Rev.* **1998**, *98*, 1–390. [[CrossRef](#)] [[PubMed](#)]
2. Cronin, L.; Müller, A. Themed issue on polyoxometalate cluster science. *Chem. Soc. Rev.* **2012**, *41*, 7325–7648.
3. Kruse, J.-H.; Langer, M.; Romanenko, I.; Trentin, I.; Hernández-Castillo, D.; González, L.; Schacher, F.H.; Streb, C. Polyoxometalate-Soft Matter Composite Materials: Design Strategies, Applications, and Future Directions. *Adv. Funct. Mater.* **2022**, *32*, 2208428. [[CrossRef](#)]
4. Li, N.; Liu, J.; Dong, B.-X.; Lan, Y.-Q. Polyoxometalate-Based Compounds for Photo- and Electrocatalytic Applications. *Angew. Chem. Int. Ed.* **2020**, *59*, 20779–20793. [[CrossRef](#)] [[PubMed](#)]
5. Xia, K.; Yamaguchi, K.; Suzuki, K. Recent Advances in Hybrid Materials of Metal Nanoparticles and Polyoxometalates. *Angew. Chem. Int. Ed.* **2023**, *62*, e202214506. [[CrossRef](#)]
6. Tahmasebi, M.; Mirzaei, M.; Frontera, A. Noble metals in polyoxometalates. *Inorg. Chim. Acta* **2021**, *523*, 120410. [[CrossRef](#)]
7. Iwase, Y.; Tomita, O.; Naito, H.; Higashi, M.; Abe, R. Molybdenum-substituted polyoxometalate as stable shuttle redox mediator for visible light driven Z-scheme water splitting system. *J. Photochem. Photobiol. A Chem.* **2018**, *336*, 347–354. [[CrossRef](#)]
8. Tomita, O.; Naito, H.; Nakada, A.; Higashi, M.; Abe, R. Mono-transition-metal-substituted polyoxometalates as shuttle redox mediator for Z-scheme water splitting under visible light. *Sustain. Energy Fuels* **2022**, *6*, 664–673. [[CrossRef](#)]
9. Suzuki, K.; Mizuno, N.; Yamaguchi, K. Polyoxometalate Photocatalysis for Liquid-Phase Selective Organic Functional Group Transformations. *ACS Catal.* **2018**, *11*, 10809–10825. [[CrossRef](#)]
10. Kikukawa, Y.; Suzuki, K.; Yamaguchi, K.; Mizuno, N. Synthesis, Structure Characterization, and Reversible Transformation of a Cobalt Salt of a Dilacunary γ -Keggin Silicotungstate and Sandwich-Type Di- and Tetracobalt-Containing Silicotungstate Dimers. *Inorg. Chem.* **2013**, *52*, 8644–8652. [[CrossRef](#)]
11. Minato, T.; Salley, D.; Mizuno, N.; Yamaguchi, K.; Cronin, L.; Suzuki, K. Robotic Stepwise Synthesis of Hetero-Multinuclear Metal Oxo Clusters as Single-Molecule Magnets. *J. Am. Chem. Soc.* **2021**, *143*, 12809–12816. [[CrossRef](#)]
12. Anjass, M.; Lowe, G.A.; Streb, C. Molecular Vanadium Oxides for Energy Conversion and Energy Storage: Current Trends and Emerging Opportunities. *Angew. Chem. Int. Ed.* **2021**, *60*, 7522–7532. [[CrossRef](#)]
13. Hayashi, Y. Hetero and lacunary polyoxovanadate chemistry: Synthesis, reactivity and structural aspects. *Coord. Chem. Rev.* **2011**, *255*, 2270–2280. [[CrossRef](#)]
14. Maruyama, T.; Namekata, A.; Sakiyama, H.; Kikukawa, Y.; Hayashi, Y. Redox Active Mixed-Valence Hexamanganese Double-cubane Complexes Supported by Tetravanadates. *New J. Chem.* **2019**, *43*, 17703–17710. [[CrossRef](#)]
15. Seliverstov, A.; Forster, J.; Heiland, M.; Unfried, J.; Streb, C. The anion-binding polyanion: A molecular cobalt vanadium oxide with anion-sensitive visual response. *Chem. Commun.* **2014**, *50*, 7840–7843. [[CrossRef](#)]
16. Meyer, R.M.; Brennessel, W.W.; Matson, E.M. Synthesis of a gallium-functionalized polyoxovanadate-alkoxide cluster: Toward a general route for heterometal installation. *Polyhedron* **2018**, *156*, 303–311. [[CrossRef](#)]
17. Meyer, R.L.; Greer, S.M.; Blake, A.V.; Cary, S.K.; Ditter, A.S.; Daly, S.R.; Li, F.; Kozimor, S.A.; Matson, E.M.; Mocko, V.; et al. Characterizing polyoxovanadate-alkoxide clusters using vanadium K-edge X-ray absorption spectroscopy. *Chem. Eur. J.* **2021**, *5*, 1592–1597. [[CrossRef](#)]
18. Dagar, M.; Corr, M.; Mckone, J.R.; Matson, E.M. Solvent mixtures for improved electron transfer kinetics of heterometallic charge carriers in nonaqueous redox flow batteries. *J. Mater. Chem. A.* **2023**, *11*, 13729–13741. [[CrossRef](#)]
19. Lee, U.; Joo, H.-C.; Park, K.-M.; Mal, S.S.; Kortz, U.; Keita, B.; Nadjo, L. Facile Incorporation of Platinum(IV) into Polyoxometalate-Frameworks: Preparation of $[\text{H}_2\text{PtIV}^{\text{V}}_9\text{O}_{28}]^{5-}$ and Characterization by ^{195}Pt NMR Spectroscopy. *Angew. Chem. Int. Ed.* **2008**, *47*, 793–796. [[CrossRef](#)] [[PubMed](#)]

20. Wang, S.-J.; Dong, W.-K.; Chen, Y.-M. Synthesis and Structural Characterization of A Single Crystal of $[\text{Na}_2(\text{H}_2\text{O})_{10}](\text{NH}_4)_3(\text{NH}_3)[\text{MoV}_9\text{O}_{28}]$. *Synth. React. Inorg. Met. Org. Chem.* **2006**, *36*, 649–653. [[CrossRef](#)]
21. Li, F.; Long, D.-L.; Cameron, J.M.; Miras, H.N.; Pradeep, C.P.; Xu, L.; Cronin, L. Cation induced structural transformation and mass spectrometric observation of the missing dodecavanadomanganate(IV). *Dalton Trans.* **2012**, *41*, 9859–9862. [[CrossRef](#)] [[PubMed](#)]
22. Kastner, K.; Forster, J.; Ida, H.; Newton, G.N.; Oshio, H.; Streb, C. Controlled Reactivity Tuning of Metal-Functionalized Vanadium Oxide Clusters. *Chem. Eur. J.* **2015**, *21*, 7686–7689. [[CrossRef](#)] [[PubMed](#)]
23. Repp, S.; Remmers, M.; Rein, A.S.J.; Sorsche, D.; Gao, D.; Anjass, M.; Mondeshki, M.; Carrella, L.M.; Rentschler, E.; Streb, C. Coupled reaction equilibria enable the light-driven formation of metal-functionalized molecular vanadium oxides. *Nat. Commun.* **2023**, *14*, 5563. [[CrossRef](#)] [[PubMed](#)]
24. Greiner, S.; Schwarz, B.; Ringenberg, M.; Dürr, M.; Ivanovic-Burmazovic, I.; Fichtner, M.; Anjass, M.; Streb, C. Redox-inactive ions control the redox-activity of molecular vanadium oxides. *Chem. Sci.* **2020**, *11*, 4450–4455. [[CrossRef](#)] [[PubMed](#)]
25. Greiner, S.; Schwarz, B.; Streb, C.; Anjass, M. Effect of heterometal-functionalization and template exchange on the redox chemistry of molecular vanadium oxides. *Chem. Eur. J.* **2021**, *27*, 13435–13441. [[CrossRef](#)]
26. Kikukawa, Y.; Kawabata, H.; Hayashi, Y. Synthesis of Cyanooxovanadate and Cyanosilylation of Ketones. *RSC Adv.* **2021**, *11*, 31688–31692. [[CrossRef](#)] [[PubMed](#)]
27. Monakhov, K.Y.; Bensch, W.; Kögerler, P. Semimetal-functionalised polyoxovanadates. *Chem. Soc. Rev.* **2015**, *44*, 8443–8483. [[CrossRef](#)]
28. Koyama, K.; Hayashi, Y.; Isobe, K. Self-assembled All-inorganic Chiral Polyoxovanadate: Spontaneous Resolution of Nitrate-incorporated Octadecavanadate. *Chem. Lett.* **2008**, *37*, 578–579. [[CrossRef](#)]
29. Greiner, S.; Hettig, J.; Laws, A.; Baumgärtner, K.; Bustos, J.; Pöppler, A.-C.; Clark, A.H.; Nyman, M.; Streb, C.; Anjass, M. A General Access Route to High-Nuclearity, Metal-Functionalized Molecular Vanadium Oxides. *Angew. Chem. Int. Ed.* **2022**, *61*, e20211454. [[CrossRef](#)]
30. Brown, I.D.; Altermatt, D. Bond-valence parameters obtained from a systematic analysis of the Inorganic Crystal Structure Database. *Acta Crystallogr.* **1985**, *41*, 244–247. [[CrossRef](#)]
31. Aureliano, M. (Ed.) *Vanadium Biochemistry*; Research Signpost Publs: Kerala, India, 2007.
32. Kato, C.; Machida, R.; Maruyama, R.; Tsunashima, R.; Ren, X.-M.; Kurmoo, M.; Inoue, K.; Nishihara, S. Giant Hysteretic Single-Molecule Electric Polarisation Switching above Room Temperature. *Angew. Chem. Int. Ed.* **2018**, *57*, 13429–13432. [[CrossRef](#)]
33. Bain, G.A.; Berry, J.F. Diamagnetic Corrections and Pascal's Constants. *J. Chem. Educ.* **2008**, *85*, 532–536. [[CrossRef](#)]
34. Chilton, N.F.; Anderson, R.P.; Turner, L.D.; Soncini, A.; Murray, K.S. PHI: A powerful new program for the analysis of anisotropic monomeric and exchange-coupled polynuclear d- and f-block complexes. *J. Comput. Chem.* **2013**, *34*, 1164–1175. [[CrossRef](#)]
35. *APEX3, SAINT, and SADABS*; Bruker AXS, Inc.: Madison, WI, USA, 2015.
36. Farrugia, L.J. WinGX suite for small-molecule single-crystal crystallography. *J. Appl. Crystallogr.* **1999**, *32*, 837–838. [[CrossRef](#)]
37. Sheldrick, G.M. *SHELXL-2018*; Universität Göttingen: Göttingen, Germany, 2018.
38. Kurata, T.; Uehara, A.; Hayashi, Y.; Isobe, K. Cyclic Polyvanadates Incorporating Template Transition Metal Cationic Species: Synthesis and Structures of Hexavanadate $[\text{PdV}_6\text{O}_{18}]^{4-}$, Octavanadate $[\text{Cu}_2\text{V}_8\text{O}_{24}]^{4-}$, and Decavanadate $[\text{Ni}_4\text{V}_{10}\text{O}_{30}(\text{OH})_2(\text{H}_2\text{O})_6]^{4-}$. *Inorg. Chem.* **2005**, *44*, 2524–2530. [[CrossRef](#)] [[PubMed](#)]
39. Baxter, S.M.; Wolczanski, P.T. Improved Synthesis, Redox Chemistry, and Magnetism of the Mixed-valence Isopolyanion $\text{V}_{10}\text{O}_{26}^{4-}$. *Inorg. Chem.* **1989**, *28*, 3263–3264. [[CrossRef](#)]
40. Roman, P.; Jose, A.S.; Luque, A.; Gutierrez-Zorrilla, J.M. Observation of a novel cyclic tetrametavanadate anion isolated from aqueous solution. *Inorg. Chem.* **1993**, *32*, 775–776. [[CrossRef](#)]

Disclaimer/Publisher's Note: The statements, opinions and data contained in all publications are solely those of the individual author(s) and contributor(s) and not of MDPI and/or the editor(s). MDPI and/or the editor(s) disclaim responsibility for any injury to people or property resulting from any ideas, methods, instructions or products referred to in the content.